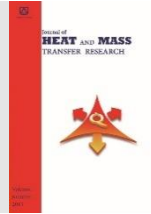




Semnan University



A New Approach for the Heat and Moisture Transfer in Desiccant Wheels Concerning Air Stream Velocity

Seyed Amir Hossein Zamzamian ^{*,a}, Hassan Pahlavanzadeh ^b,
Mohamad Reza Omidkhah Nasrin ^b

^a Energy Department, Materials and Energy Research Center (MERC), Karaj, Iran.

^b Faculty of Chemical Engineering, Tarbiat Modares University, Tehran, Iran.

PAPER INFO

Paper history:

Received: 2022-10-04

Revised: 2023-01-28

Accepted: 2023-02-11

Keywords:

Desiccant wheel;
Explicit program;
Heat transfer;
Mathematical model;
Mass transfer.

ABSTRACT

Many investigators have presented mathematical work on desiccant wheels but there is a considerable discrepancy between published values and experimental values. A mathematical model based on the two-dimensional Navier-Stokes equation has been derived to show the dehumidification trend of desiccant dehumidifier concerning air stream velocity. In this model the effect of air stream velocity on wheel performance as a momentum equation combined with heat and mass transfer has been studied.

The current model is capable of predicting the transient and steady-state transport in a desiccant wheel. It reveals the moisture and temperature in both the airflow channels and the sorbent felt, in detail, as a function of time. The predicted results are validated against the data taken from experimental results, with reasonable accuracy. Therefore, the numerical model is a practical tool for understanding and accounting for the complicated coupled operational process inside the wheel. Consequently, it is useful for parameter studies.

DOI: [10.22075/jhmtr.2023.28610.1395](https://doi.org/10.22075/jhmtr.2023.28610.1395)

© 2022 Published by Semnan University Press. All rights reserved.

1. Introduction

In the desiccant cooling process, which is a new kind of refrigeration method, the fresh air is dehumidified and then sensibly and evaporatively cooled before being sent to the conditioned space [1]. Desiccant-enhanced air conditioning equipment has exhibited both the capability to improve humidity control and the potential to save energy costs by lowering the latent energy requirement of the supply air stream. Controlling temperature and humidity within a conditioned space is important for a wide variety of applications. Desiccant dehumidifier, running in open cycle, can be driven by low-grade heat sources, e.g. solar energy, waste heat and natural gas. A procedure for the energy and exergy analyses of open-cycle desiccant cooling systems have been developed and it has been applied to an experimental unit operating in ventilation mode with natural zeolite as the desiccant [2]. Beccali et al. has presented a simple model to

evaluate the performance of rotary desiccant wheels based on different kind of solid desiccants e.g. silica gel. The 'Model 54' has been derived from the interpolation of experimental data obtained from the industry and the correlations developed for predicting outlet temperature and absolute humidity. The 'Model 54' consists of 54 coefficients corresponding to each correlation for outlet absolute humidity and temperature and it is found that the model predicts very well the performance of silica gel desiccant rotor. Then a psychro-metric model has been presented to obtain relatively simple correlations for outlet temperature and absolute humidity. The developed psychro-metric model is based on the correlations between the relative humidity and enthalpy of supply and regeneration air streams [3]. Then the update on the desiccant wheel models developed. It is to be mentioned that the psychro-metric model is valid only for the desiccant wheel running with identical volume

*Corresponding Author: Seyed Amir Hossein Zamzamian.
Email: azamzamian@merc.ac.ir

air flows in supply and regeneration side. When system runs with volume air flow ratio between supply and regeneration side, the model needs further modification. Some correction factors in order to update the model for correct prediction of the temperature and humidity of processed air at the outlet of desiccant wheel have been developed and also incorporated [4]. Many mathematical models on the rotary desiccant dehumidifier have been proposed. Maclaine-Cross IL presented that a finite difference computer program, MOSHMX, can be developed based on a detailed numerical analysis [5]. Barlow presented that DESSIM could be written where the dehumidifier was discretized and each node was treated as a counter flow heat and mass exchanger in which both the heat and mass transfer are assumed to be uncoupled [6]. Then Collier and Cohen developed ET/DESSIM that is more accurate than DESSIM [7]. The mathematical model by finite difference method to predict the performance and to optimize the operation parameters of rotary desiccant wheels have been proposed. The effect of the rotational speed on the performance of an adiabatic rotary dehumidifier was parametrically studied, and the optimal rotational speed was determined by examining the outlet adsorption side humidity profiles and humidity wave front inside the desiccant dehumidifier [8]. The mathematical model of a rotary desiccant wheel have been used to calculate the performance of stationary or rotary bed and transient or steady state operation is founded by considering some of the key components [9]. This is helpful for predicting the performance and evaluating the benefits of rotary desiccant wheels concerning the complicated heat and mass transfer in the rotary desiccant matrix that was suggested [10-11]. The continuity and energy conservation equations for the transient coupled heat and mass transfer using a finite differential model have been established and solved, that the present study was mostly derived from this research [12-13]. A simple mathematical model for explanation of the rotary desiccant wheel, in which the optimum rotational speed for achieving the maximum performance offered have been presented [14]. On the other hand, a mathematical model for a fixed desiccant bed to show the dehumidification trend of desiccant dehumidifier concerning Ackermann correction factor with no rotation have been derived [15]. As mentioned, in all activities like the above references, the attitude, model solution and outcome analysis are much different from this research. There are various numerical modeling presented of rotary wheels and also calculation of mass and heat transfer in those models by various researchers [8-9]. In these activities the effect of conduction within the desiccant wall has been considered. Also in this model an optimized velocity for exchangers has been determined. Experimental measurements on rotary silica gel exchangers has been presented in these

researches and by using temperature distribution within wheel, an experimental statement for the optimized velocity of rotation has been suggested. They have some suggestions for analysis of exchangers or silica gel rotary wheels by using psychro-metric chart. Their focus is mainly on the understanding of the measure of mass transfer in silica gel rotary desiccant systems simply or by experimental parametric analysis, and also their experimental measurements has been done on silica gel desiccant wheel. As a general result, one can say that the type and atmosphere of these works are completely different [8-11].

Studies in recent years have been necessary to improve the system's performance and reliability and reduce their costs and also to enhance the commercial competitiveness of desiccant dehumidification systems and expand their market [16-20]. For example, the one-dimensional model by using MATLAB programing to simulate the desiccant wheel has been presented when it was combined with the direct evaporative cooling, or indirect evaporative cooling, or hybrid desiccant cooling systems then it has compared between their performances [16]. An experimental comparison between the fully and annular packed beds by Adding a new configuration that integrating each of them with oscillated helical coil heat pipes have been done [17]. Also the effect of channel geometry of the desiccant wheel on its performance has been studied and that in this case, Five types of channels have been examined (triangular, square, hexagonal, sinusoidal-1, and sinusoidal-2) [20].

In Table 1 and Table 2 some of the previously investigated solid desiccant dehumidifier packed bed configurations including targets and some approaches have been summarized. In this regard, the detailed discussion of the current designs configurations and the main differences between them may help future researchers to come up with novel, innovative designs, to overcome the system's drawbacks and make them actual viable alternative competitors in the dehumidification market [33].

Of course, it should be noted that this study was conducted with a time interval from the previous research. This is because some theoretical studies and experimental researches have been completed. Finally, the ultimate goal of this study is to develop a new mathematical explicit model to analyze desiccant performance. With the implementation of a control volume technique, difference equations have been developed which were in turn used in the derivation of the governing differential equations for momentum in the air stream and also for heat and mass transfer both within the desiccant and in the air stream. These finite difference equations were solved using a quasi-central finite difference scheme. Boundary and initial conditions, Ackermann correction factor, thickness of desiccant matrix, air stream velocity and density,

rotation speed, angle of regeneration section are examples of the parameters that have been changed throughout the analysis of each total mass, enthalpy

(energy) and momentum changes. The effects of such parameter changes have been investigated as well.

Table 1. Comparative study of some previous solid desiccant packed bed investigations.

Target	Desiccant Kind
Theoretical and experimental investigations of 5 different values of diameter ratio for a hollow cylindrical shape used as a radial flow single-stage solid desiccant dehumidifier [21].	Silica Gel
Theoretical and experimental investigations of an eight-layer silica gel single-stage packed bed system were employed to study the influence of configuration and operational parameters on efficiency [22].	Silica Gel
A single-stage single-packed bed was used to experimentally analyze the efficiency of the desiccant bed for radial flow [23].	Activated Alumina
Experimental and theoretical examinations for a hollow packed bed to simulate the transient combination heat and mass transfer [24].	Silica Gel
Theoretical and experimental investigation for two packed beds assembly to simulate the thermal swing adsorption cycle [25].	Silica Gel
Introducing an intercooler heat exchanger between two sections of a single packed bed. Theoretical and experimental investigation for the intercooler effect [26].	Silica Gel
Experimental comparison between two different configurations. The first one is a traditional axial packed bed and the second is a heat exchanger with desiccant granules inside the fin gaps [27].	Silica Gel
Experimental investigation of a fixed double bed dehumidifier using two finned tube heat exchangers with desiccant granules between its fins and actuated shutters to direct the airflow [28].	Silica Gel
Introducing a tool for accurate prediction of the thermal performance of a single-stage packed bed [29].	Silica Gel
A humidifier was used to increase the indoor humidity in typical winter conditions in Italy [19].	Silica Gel
A novel MFBDD system was designed and experimentally studied [30].	Silica Gel
Prediction of the characteristics of the transient mass and heat transfer of the desorption process of a packed bed using a CFD model [31].	Silica Gel
Adding a water heating and cooling device to Shamim's configuration [30]. Calculating numerically the transient heat and mass transfer, optimization for all parameters [18].	Silica Gel
An experimental investigation of a Z-annular packed bed with three diametrical ratios that offered radial distribution of airflow [32].	Silica Gel
An experimental comparison between the fully and annular packed beds. Adding a new configuration by integrating each of them with oscillated helical coil heat pipes [17].	Silica Gel

Table 2. Comparison of the Approaches of different solid desiccant dehumidifiers

Approaches	Regeneration Method
The adsorption period for appropriate performance was found to be about 15 min for a 7.2 diameter ratio. This period decreased with increasing the bed diameter ratio or the airflow rate [21].	Electrical heater
The inlet temperature was the main parameter that affects the desorption rates. After an hour, the accumulated water quantity between the first and last layers of the bed might range from 200 to 400 % based on the inlet condition [22].	Electrical heater
This system reached very low levels of 1.2 g/kg at inlet conditions of air humidity from 18.7 to 12.5 g/kg [23].	Electrical heater
Desorption time and temperature had a large effect on the adsorption process performance. Pre-cooling or cooling the adsorption bed enhanced the cycle performance [24].	Electrical heater
By extending the length of the bed, the humidity ratio of the outlet air decreased. The cycle performance was enhanced by raising the velocity of the inlet air [25].	Electrical heater
The optimum intercooler position was found to be within a range of 0.45 to 0.65 of the total bed lengths for a bed length range of 5 to 100 cm. For a high air flow rate desiccant bed, the intercooler had no effect [26].	Electrical heater
Using finned tube air-water heat exchanger enhanced dehumidification performance as a result of cooling the desiccant material during the adsorption process [27].	Hot water heat exchanger
This system could use low-grade heat supply temperature sources below 55° C. The Specific Cooling Power (SCP) was ranged between 30 and 180 (W kg ⁻¹ of adsorbent) [28].	Hot water heat exchanger
A small fin pitch (4 mm) had the best performance. A new semi-empirical formula is used as an accurate prediction tool of the system performance with the variation of the operating condition [29].	Hot water heat exchanger.
The regeneration bed increased the humidity ratio of the building supplied air from 1.5 g kg ⁻¹ to 5.3 - 6.1 g.kg ⁻¹ and temperature of 60° C [19].	Heating coil
This novel configuration decreased the pressure drop of the bed by approximately 98% and increased the average adsorption capacity by 36% compared to a conventional desiccant dehumidification system [30].	Dry nitrogen
The theoretical results showed an agreement with the experimental results obtained in [30-31].	Dry nitrogen
Adding heating and cooling water enhanced the system performance. Adsorption and desorption isotherms have a significant influence on the system performance [18].	Heating water
The best performance of the Z-annular configuration was achieved by lowering the temperature to around 4.22 to 5.47° C below that of the standard bed. The pressure drop in the Z-annular bed is larger than that in the standard packed bed [32].	300W heating element.
The annular bed had an adsorption rate larger than the full bed. The temperature reduction was between 20° C to 3° C due to using a heat pipe [17].	300W heating element.

2. Mathematical Model of a Two Dimensional Rotary Wheel

2.1 Basic Equations

A rotary regenerative desiccant wheel is shown in figure 1(a). It is a rotary cylindrical wheel of length L and diameter d_w and it is divided into two sections: adsorption section (angle fraction ϕ_0) and regeneration section (fraction $1-\phi_0$), where the adsorption and regeneration air streams are in a counter flow arrangement. The wheel generally consists of a matrix of numerous flow channels which have, depending on the manufacturing process, a rectangular, triangular or sinusoidal shape. The channel walls are parallel to the axis of the wheel, and are made of composite materials which have a desiccant content of 0.7 -0.8.

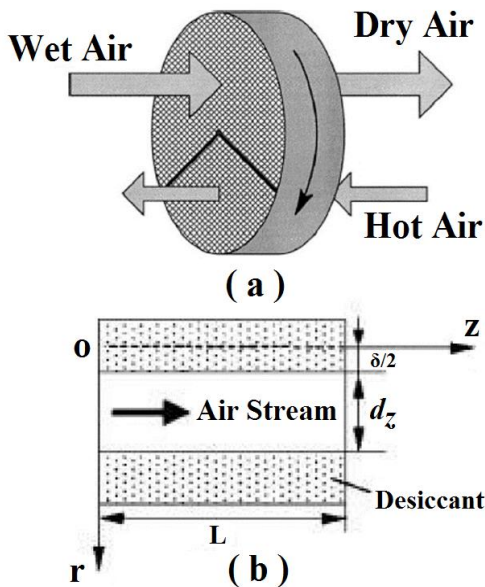


Figure 1. Schematic of the desiccant wheel showing (a) the entire wheel, (b) a side view of one of the ducts

It is assumed that the velocity of air stream and the diameter of micro channels effect on desiccant performance. The rotary wheel is a total enthalpy exchanger when it operates as a revolving exchanger circulating between two opposing air streams. Four equations concerning water content balance and energy conservation are used to describe the complicated heat and mass transfer occurring in moisture adsorption and regeneration and one equation is used to describe momentum. As already mentioned, in the previous studies the specifications of the dehumidification desiccant wheel have been completely presented [34-35]. In terms and the structure of governing equations and to solve the model, in the numerical examination of an unsteady thermo-solutal mixed convection when the extra mass and heat diffusions, there have been some similarities to work. [36].

For simplicity, some assumptions are made:

1. Two dimensional air stream flow is considered.
2. The axial heat conduction and mass diffusion in the fluid are neglected.
3. Effect of centrifugal force is neglected due to low rotation speed of the rotary dehumidifier
4. No leakage takes place between dehumidification and regeneration sections.
5. Heat and mass transfer in radial direction is not taken into consideration.
6. The thermodynamic properties in the solid are constant and uniform.
7. Shell of the rotary dehumidifier satisfies the insulated condition.
8. Velocity profile is one dimensional and considerable along z direction.

Consequently, the model used in this study is transient and two dimensional. Heat and mass conservation for the air stream

$$\frac{\partial(\rho_{da}Y)}{\partial \tau} + \omega \frac{\partial(\rho_{da}Y)}{\partial \phi} + \frac{\partial(\rho_{da}Yu)}{\partial z} = K_Y \cdot f_v (Y_w - Y) \tag{1}$$

Conservation of energy for the process air:

$$\frac{\partial(\rho_{da}C_{pe}t)}{\partial \tau} + \omega \frac{\partial(\rho_{da}C_{pe}t)}{\partial \phi} + \frac{\partial(\rho_{da}uC_{pe}t)}{\partial z} = A_f \cdot \alpha \cdot f_v (t_w - t) + K_Y \cdot f_v (Y_w - Y) C_{pv} t \tag{2}$$

Conservation of water content for the absorbent:

$$\frac{\partial W}{\partial \tau} + \omega \frac{\partial W}{\partial \phi} - D_{eff} \left[\frac{1}{r} \frac{\partial^2 W}{\partial \phi^2} + \frac{\partial^2 W}{\partial z^2} \right] = \frac{K_Y \cdot f_v}{\rho_w} (Y - Y_w) \tag{3}$$

Conservation of energy for the absorbent:

$$\frac{\partial t_w}{\partial \tau} + \omega \frac{\partial t_w}{\partial \phi} - \frac{\lambda}{\rho_w (C_{pw} + WC_{pl})} \cdot \left[\frac{1}{r} \frac{\partial^2 t_w}{\partial \phi^2} + \frac{\partial^2 t_w}{\partial z^2} \right] = \frac{1}{\rho_w (C_{pw} + WC_{pl})} [A_f \cdot \alpha \cdot f_v (t - t_w) + K_Y \cdot f_v (Y - Y_w) Q] \tag{4}$$

Momentum equation for the process air:

$$\frac{\partial(\rho_g \cdot u)}{\partial \tau} + \frac{\partial(\rho_g \cdot u^2)}{\partial z} = \frac{\Delta P}{L} \tag{5}$$

2.2 Auxiliary relations

The Ackerman heat transfer correction factor for mass transfer fluxes in phase j [37]:

$$A_f = \frac{C_f}{e^{C_f} - 1} \tag{6}$$

$$C_f = \frac{\sum_i J_{i,j} C_{pi,j}}{h_j} \quad (j = g \text{ or } l) \tag{7}$$

For air stream process:

$$C_f = \frac{J \cdot C_{pa}}{h} \tag{8}$$

$$J = K_Y (Y_w - Y) \quad (9)$$

Mass transfer coefficient is calculated by acquiring experimental data. For air and water system, relationship between mass and heat transfer coefficient is given below:

$$K_Y = \frac{\alpha}{C_{p_e} Le} \quad (10)$$

where Le is Lewis number that for air and water system is equal to one. Heat transfer coefficient is obtained by optimization of experimental and theory data.

Table 1. Experimental condition to obtain heat and mass transfer coefficient

Variable	Environmental Condition	Input data
Relative humidity (%)	25	35.5
Temperature(C)	27.6	30.2
Velocity (m/s)	-	4.6

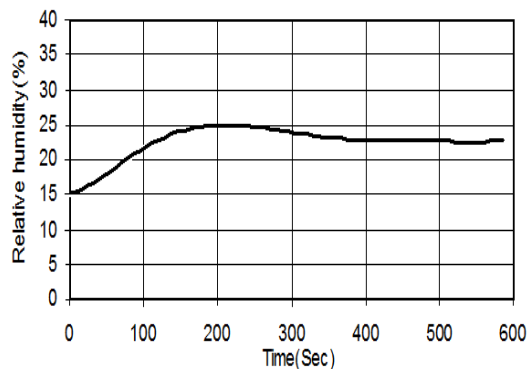


Figure 2. Relative humidity versus time at experimental condition

Mathematical correlation for the curve in figure 2 is given below:

$$RH_{EXP} = 3 \times 10^{-7} \tau^3 - 3 \times 10^{-4} \tau^2 + 0.1066 \tau + 14.072 \quad (11)$$

where RH_{EXP} is outlet relative humidity which is calculated experimentally.

By using error function and optimization between experimental and theory data, final correlations for heat and mass transfer coefficient are obtained as below:

$$\alpha = 0.671 m_i Re^{-0.51} (C_{p_a} + Y.C_v) \quad (12)$$

$$K_Y = 0.704 m_i Re^{-0.51} \quad (13)$$

For enthalpy calculations, different correlations were developed corresponding to different kinds of desiccant wheel, which are as follows for two types of Silica Gel [3]:

$$\text{Type I} \quad h = 0.312 h_{reg} + 0.8688 h_m \quad (14)$$

$$\text{Type II} \quad h = 0.1148 h_{reg} + 0.8852 h_m - 0.9474 \quad (15)$$

Enthalpy in the regeneration and inlet side of the wheel calculate by:

$$h = C_{p_a} t + C_{p_v} t Y \quad (16)$$

In the equations (12-16), the air humidity ratio near the wall of adsorbent is unknown; Therefore, three auxiliary relations are needed:

$$Y_w = 0.62198 \frac{RH}{\left(\frac{P_{atm}}{P_{ws}} + RH\right)} \quad (17)$$

Experimental value for silica gel relative humidity expression [10]:

$$RH = 0.0078 - 0.05759W + 24.1655W^2 - 124.478W^3 + 204.226W^4 \quad (18)$$

$$\ln(P_{ws}) = \frac{\lambda_1}{(t_w + 273.15)} + \lambda_2 + \lambda_3(t_w + 273.15) + \lambda_4(t_w + 273.15)^2 + \lambda_5(t_w + 273.15)^3 + \frac{\lambda_6}{\ln(t_w + 273.15)} \quad (19)$$

where the coefficients are as follows:

$$\begin{aligned} \lambda_1 &= -5800.2206 & \lambda_2 &= 1.3914933 \\ \lambda_3 &= -0.04860239 & \lambda_4 &= 0.41764768 \times 10^{-4} \\ \lambda_5 &= -0.14452093 \times 10^{-7} & \lambda_6 &= 6.5459673 \end{aligned}$$

Heat transfer coefficient is given below [11]:

$$\alpha = 0.671 m_i Re^{-0.51} (C_{p_a} + Y.C_v) \quad (20)$$

The adsorption heat of regular density silica gel is calculated by [11]:

$$Q = \begin{cases} -13400 W + 3500, & W \leq 0.05 \\ -1400 W + 2950, & W > 0.05 \end{cases} \quad (21)$$

The surface diffusivity for adsorption of silica gel is given as [11]:

$$D_{eff} = D_0 \left[-0.974 \times 10^{-3} \frac{Q}{t_w + 273.15} \right] \quad (22)$$

In this study, regular density (RD) silica gel is chosen as desiccant and several auxiliary equations are

appended meanwhile. The calculation conditions of the base case are listed.

For regeneration section, if $2\pi - \phi R \leq \phi < 2\pi$, then

$$Y_{in} = Y_2, \quad t_{in} = t_2 \quad (23)$$

For dehumidification section, $0 \leq \phi < 2\pi - \phi R$, then

$$Y_{in} = Y_1, \quad t_{in} = t_1 \quad (24)$$

In addition, the periodic boundary conditions are given as:

For air stream:

$$Y(0, z, \tau) = Y(2\pi, z, \tau) \quad (25)$$

$$t(0, z, \tau) = t(2\pi, z, \tau) \quad (26)$$

For desiccant bed:

$$W(0, z, \tau) = W(2\pi, z, \tau) \quad (27)$$

$$t_w(0, z, \tau) = t_w(2\pi, z, \tau) \quad (28)$$

If the transient problem is taken into consideration, the initial conditions are also necessary:

For desiccant,

$$W(\phi, z, 0) = W_0, \quad t_w(\phi, z, 0) = t_0 \quad (29)$$

For dehumidification air stream, $0 \leq \phi < 2\pi - \phi R$,

$$Y(\phi, z, 0) = Y_1, \quad t(\phi, z, 0) = t_1 \quad (30)$$

For regeneration air stream, $2\pi - \phi R \leq \phi < 2\pi$,

$$Y(\phi, z, 0) = Y_2, \quad t(\phi, z, 0) = t_2 \quad (31)$$

here, t_1 and t_2 denote the inlet air temperatures for dehumidification section and regeneration section, respectively, t_0 and Y_0 stand for temperature and humidity ratio at initial conditions, and Y_1, Y_2 stand for inlet air humidity for dehumidification and regeneration sections. Momentum equation boundary conditions for the process air:

Adsorption:

$$u(0, \tau) = u_0 \quad (32)$$

$$u(L, \tau) = u_a \quad (33)$$

Regeneration:

$$u(0, \tau) = u_0 \quad (34)$$

$$u(L, \tau) = u_r \quad (35)$$

2.3 Experimental Setup

In figure 3, the experimental setup of a solid adsorption cooling system with the cooling capacity of about 2 Cooling Ton and in figure 4, a schematic design of an adsorption cooling system provided with a rotary desiccant wheel is shown. Generally, the system consists of a cooling cycle and a desiccant wheel. Inlet air can be provided from point 1 or point 1'. If the air flows from point 1, it passes through a filter to lose any probable dust. In point 2, the filtered air is starting to flow through the desiccant wheel. The desiccant wheel rotates by an AC motor with a changeable rotation control system. Using this system, one can set the rotary speed according to the desired conditions to increase the quality of regeneration process. In point 3, air loses moisture by the adsorbent, and because of the condensation of moisture, temperature of the air increases. Then by passing the air through the evaporator of cooling cycle, its temperature reduces to the desired measure. The cooled air flows into the desired room and cools it which is point 4. For regeneration of the desiccant, outdoor air is consumed. At point 5, air flows into the regeneration chamber of desiccant. Air stream passes through an electric heater and its temperature rises. As a result, at point 6, there is a hot stream of air which is suitable to regenerate the desiccant. As the hot air passes through the desiccant, releases the moisture adsorbed by the desiccant and carries it out. Because of this process, at point 7, air temperature reduces a little but gains moisture. There are compressors and condenser of the cooling cycle at the end part of the system. A fan is used to cool the condenser which is cooled by the mandatory air stream made by the fan. In this research which is done to reach the above mentioned goals, only experimental test is done on the rotary desiccant wheel. Then, experimental conditions for inlet and outlet streams are like the ones in figure 5.



Figure 3. Photo of the solid adsorption cooling system equipment and wheel for doing experiments

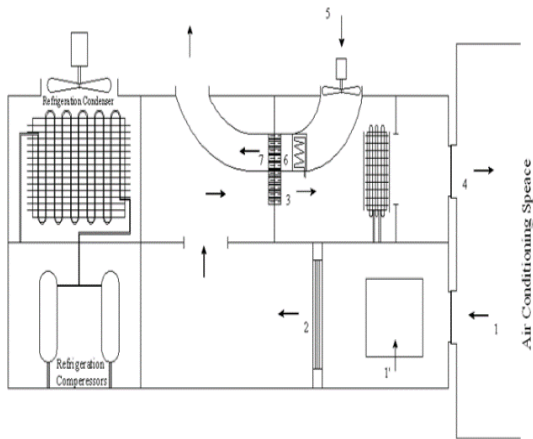


Figure 4. A schematic design of the full adsorption cooling system

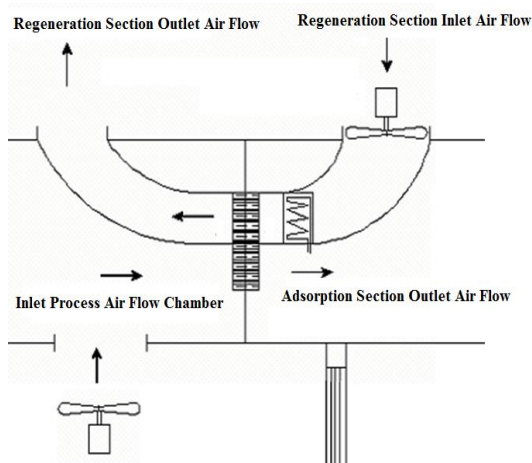


Figure 5. Schematic picture of the experimental system

3. Results and discussion

3.1 Model validation

In order to validate the current model, several comparisons are conducted in this section between measured results derived from experimental investigation and the ones predicted by the current model. The wheel used in the comparison is a commercially available desiccant dehumidification wheel. The dimensions of the wheel are listed in Table 2. The cross-area of each elementary channel is assumed to be 0.81 mm², and the number of gross elements is assumed as 14,600. In addition, the thickness of the adsorption is 0.1mm. The initial conditions in the cases are 20°C temperature and 25% relative humidity (or 3.69 g/kg-DA). The moisture content in the desiccant is in equilibrium with the ambient condition and is determined by Eq. 14 on the basis of inlet air temperature and humidity. The inlet parameters, including temperature and humidity ratio, are considered as a function of time and gradually increased from the ambient condition to the set points. The delay time is around 4 min in accordance with the experimental data. Wheel rotational speed is

10 rph, and airflow rate for both the adsorption and regeneration sections is 0.897 m³/s.

Table 2. Geometrical characteristics of desiccant wheel

Wheel dimensions	Unit	Value
Wheel depth	m	0.2
Wheel diameter	m	0.2
Wheel volume	m ³	0.178
Adsorption face area	m ²	0.593
Regeneration face area	m ²	0.593

Figures 6-7 plots the comparison of predicted and measured parameters, such as outlet air adsorption temperature and relative humidity or moisture removal capacity (MRC), in a transient process. In this case, adsorption inlet temperature is 31°C and regeneration inlet temperature is 88°C. Both inlet air humidity ratios are 12.5 g/kg-DA, which represent 45.1 and 3.1% RM, respectively. From Fig. 6 and Fig. 7, the prediction approaches the steady state a little more quickly than of the actual experiment. This is because the prediction is conducted under ideal operating conditions, while the actual system is affected by many uncertain factors, e.g. unstable heating and flow leakage

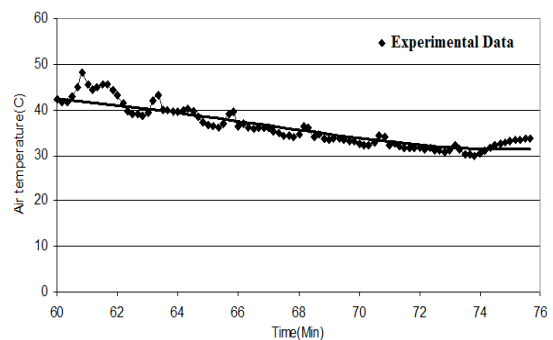


Figure 6. Outlet Air temperature versus time at experimental condition and theoretical model

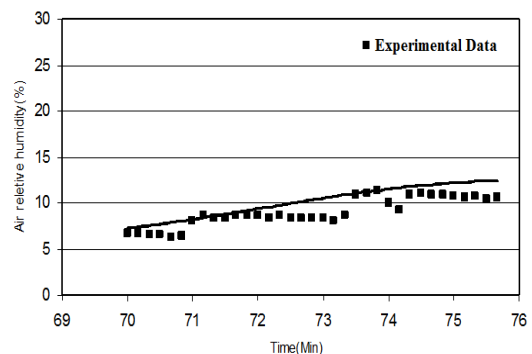


Figure 7. Outlet Relative humidity versus time at experimental condition and theoretical model

Figure 8 shows the comparison of predicted and measured air stream velocity in a steady state. In this case, regeneration inlet temperature is still 88°C, but adsorption inlet temperature is 35°C. The result illustrates that the predicted adsorption outlet air stream velocity is slightly more than the velocity in the experimental data. The difference is between 1 and 2 m/s. The moisture removal capacity is close to that of the experimental result. The regeneration outlet temperature is not compared because data were unavailable.

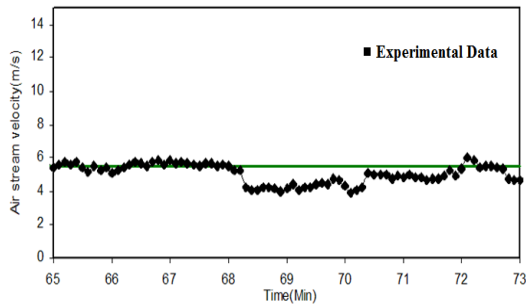


Figure 8. Air stream velocity versus time at experimental condition and theoretical model

3.2 Periodic profiles

The model can reveal the moisture and temperature morphology in both the airflow channel and the sorbent in detail. A typical periodic profile of the thermal parameters of an element in a steady state, including temperature and moisture content, is shown in Fig.9 to Fig.11. The adsorption inlet humidity ratio is 75% in the case shown. These figures show periodic performance in one and two complete rotation of the wheel. Second periods are different from the first one because of the bed temperature. When hot air stream enter the wheel from other side of the channel, bed temperature raises and consequently, the bed water content decreases. The periodic profile is formed as a result of the periodic alternation between adsorption and regeneration. The numerical model provides a strong tool for understanding and accounting for the complicated coupled processes inside the wheel.

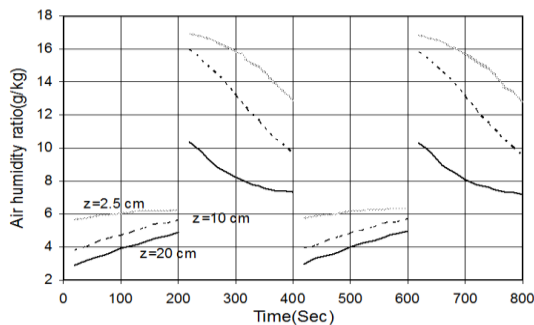


Figure 9. Periodic profile of predicted transient parameters of an element in a steady state for air humidity ratio

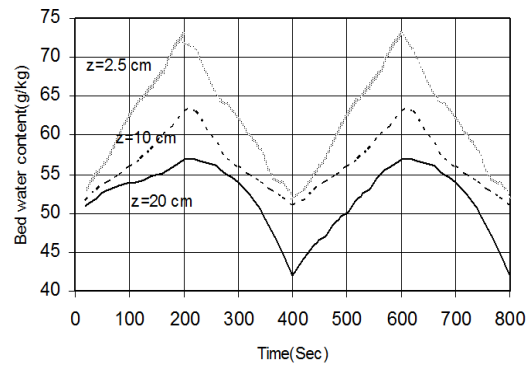


Figure 10. Periodic profile of predicted transient parameters of an element in a steady state for bed water content

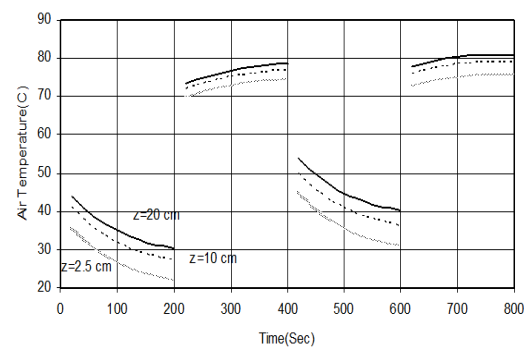


Figure 11. Periodic profile of predicted transient parameters of an element in a steady state for air temperature

3.3 Discussion on air stream velocity

Alongside the canal of desiccant wheel, since the temperature is more effective as the air temperature increases and reduces moisture, air stream velocity increases which can be proved by experimental results too. That is, with comparing the figures 12 and 13, air stream velocity increases from the initial amount of 4.6 m/s to the final amount of 6.5 m/s. But air stream velocity decreases in each section as time passes, since temperature which is the effective parameter decreases in each section as time passes (because gas is cooled)

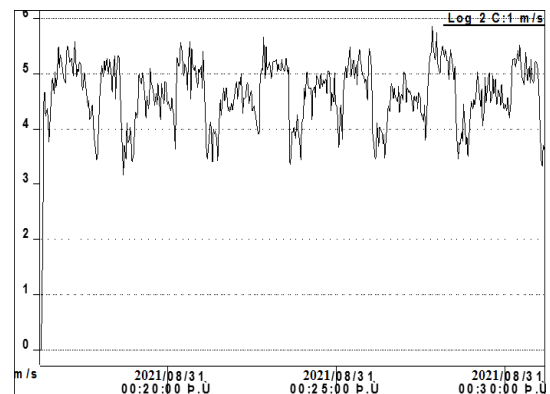


Figure 12. Velocity of inlet air stream versus time according to the experiment conditions

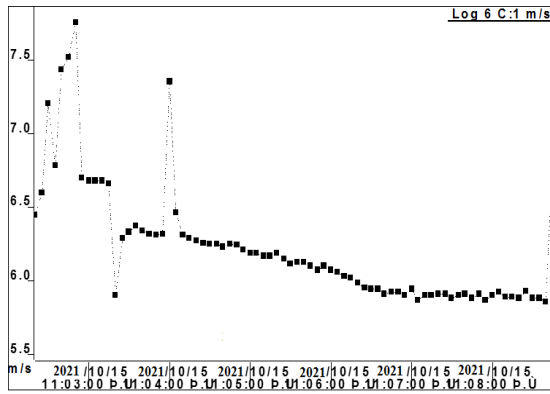


Figure 13. Experimental data for velocity of outlet air stream through wheel (m/s) versus time (s) which is recorded from 11:03 to 11:08 by the instrument

4. Conclusion

A mathematical model based on the two-dimensional Navier-Stokes equation was developed in an effort to investigate the transport phenomena occurring within the porous sorbent and the airflow channels in a desiccant wheel. These governing equations include those terms due to heat and mass transfer within the sorbent and between the sorbent and the flow channel. The model can reveal the moisture and temperature in both the airflow channel and the sorbent in detail as a function of time. The results predicted by the current model are further validated with reasonable accuracy against data taken from experimental results. Therefore, the numerical model is assumed to be a positive tool that accounts for the transport phenomena within the wheel and, consequently, is ideal for parameter studies that can lead to design optimization. As a demonstration of its utility, the model is employed to study the effect of periodic rotational of the wheel. The results illustrate that the rotational of the wheel influences both the transient and the steady-state performance of a desiccant wheel.

Acknowledgements

This study has been conducted based on a research Grant No. 528706 in the Materials and Energy Research Centre (MERC), which is hereby appreciated.

Nomenclature

A_f	Ackermann heat transfer correction factor
C_{pa}	Specific heat of air ($J \cdot kg^{-1} \cdot K^{-1}$)
C_{pl}	Specific heat of water ($J \cdot kg^{-1} \cdot K^{-1}$)
C_{pw}	Specific heat of desiccant ($J \cdot kg^{-1} \cdot K^{-1}$)
C_{pv}	Specific heat of water vapor ($J \cdot kg^{-1} \cdot K^{-1}$)
C_{fg}	Latent heat of water ($J \cdot kg^{-1}$)
C_{pz}	Specific heat of supporting materials ($J \cdot kg^{-1} \cdot K^{-1}$)

C_{pe}	Equivalent specific heat ($J \cdot kg^{-1} \cdot K^{-1}$)
D_{eff}	Effective diffusivity of desiccant ($m^2 \cdot s^{-1}$)
D_0	Effective diffusivity of desiccant at standard condition ($m^2 \cdot s^{-1}$)
f_v	Ratio of desiccant surface area to volume ($m^2 \cdot m^{-3}$)
f_s	Ratio of free flow area to section area of rotary wheel
h	Enthalpy ($J \cdot kg^{-1}$)
h_{in}	Enthalpy inlet or in the process side of the wheel ($J \cdot kg^{-1}$)
h_{reg}	Enthalpy in the regeneration side of the wheel ($J \cdot kg^{-1}$)
J	Mass flux ($kg \cdot m^{-2} \cdot s^{-1}$)
K_Y	Coefficient of mass convection ($kg \cdot m^{-2} \cdot s^{-1}$)
L	Thickness of the desiccant matrix (m)
m_i	Mass flow air per unit section area wheel ($kg \cdot m^{-2} \cdot s^{-1}$)
M_w	Desiccant mass per unit volume ($kg \cdot m^{-3}$)
M_z	Mass of supportive structure per unit volume ($kg \cdot m^{-3}$)
P_{ws}	Saturation pressure (Pa)
ΔP	Pressure drop in desiccant matrix channel (Pa)
P_{atm}	Atmospheric pressure (Pa)
Q	Adsorption heat ($J \cdot kg^{-1} \cdot water$)
r_1	Radius of the matrix axis (m)
r_2	Radius of the rotary wheel (m)
RH	Relative humidity
t	Temperature of air ($^{\circ}C$)
t_w	Temperature of desiccant ($^{\circ}C$)
T_{db}	Dry bulb temperature of the air ($^{\circ}C$)
u	Air stream velocity ($m \cdot s^{-1}$)
u_a	Velocity of dehumidification air stream ($m \cdot s^{-1}$)
u_r	Velocity of regeneration air stream ($m \cdot s^{-1}$)
W	Water content of desiccant ($kg_{water} \cdot kg^{-1}_{adsorbent}$)
Y	Humidity ratio ($kg_{moisture} \cdot kg^{-1}_{dry air}$)
Y_w	Humidity ratio near desiccant wall ($kg_{moisture} \cdot kg^{-1}_{dry air}$)

Greek symbols

α	Coefficient of heat transfer ($W \cdot m^{-2} \cdot K^{-1}$)
ρ_{da}	Dry air density ($kg \cdot m^{-3}$)
ρ_g	Wet air density ($kg \cdot m^{-3}$)
ρ_w	Water density ($kg \cdot m^{-3}$)
η	Dehumidifier performance
λ	Thermal conductivity of desiccant ($W \cdot m^{-1} \cdot K^{-1}$)
τ	Time (sec)
ω	Rotation speed (sec^{-1})
r, ϕ, z	Polar coordinates
ϕ_R	Angle of regeneration section

References

- [1] Staton, J.C., Scott, E.P., Kander, R.G., Thomas, J.R., 1998. Heat and mass transfer characteristics of desiccant polymers. M.S. Thesis, Virginia Polytechnic Institute and State University, Virginia, USA.
- [2] Konogula, M., Carpinlioglu, Ö.M., Yildirim, M., 2004. Energy and exergy analysis of an experimental open cycle desiccant cooling system. *Applied Thermal Engineering*, 24, pp. 919-932.
- [3] Beccali, M., Adhikari, R.S., Butera, F., Franzitta, V., 2004. Update on desiccant wheel model. *International Journal of Energy Research*, 28, pp. 1043-1049.
- [4] Beccali, M., Butera, F., Guanella, R., Adhikari, R.S., 2003. Simplified models for the performance evaluation of desiccant wheel dehumidification. *International Journal of Energy Research*, 27, pp. 17-29.
- [5] Maclaine-Cross, I.L., 1988. Proposal for a desiccant air conditioning system. *ASHRAE Transaction*, 94, pp.1997-2009.
- [6] Barlow, R.S., 1982. Analysis of Adsorption Process and of Desiccant Cooling System; a Pseudo-Steady-State Model for Coupled Heat and Mass Transfer. Solar Energy Research Institute TR, pp. 631-1330.
- [7] Collier, R.K., Cohen, B.M., 1991. An analytic investigation of methods for improving the performance of desiccant cooling system. *ASME Journal of Solar Energy Science and Engineering*, 113, pp. 157-163.
- [8] Zheng W, Worek WM, 1993. Numerical simulation of combined heat and mass transfer processes in a rotary dehumidifier. *Numerical Heat Transfer*, 23, pp. 211-232.
- [9] Zheng, W., Worek, W.M., Novosel, V., 1995. Performance optimization of rotary dehumidifiers. *ASME Journal of Solar Energy Science and Engineering*, 117, pp. 40-44.
- [10] Zhang, H.F., Yu, J.D., Liu, Z.S., 1996. The research and development of the key components for desiccant cooling system. *World Renewable Energy Congress*, pp. 653-656.
- [11] Zhang, L.Z., Niu, J.L., 2002. Performance comparisons of desiccant wheels for air dehumidification and enthalpy recovery. *Applied Thermal Engineering*, 22, pp. 1347-1367.
- [12] Dai, Y.J., Wang, R.Z., Zhang, H.F., 2001. Parameter analysis to improve rotary desiccant dehumidification using a mathematical model. *International Journal of Thermal Science*, 40, pp. 400-408.
- [13] Dai, Y.J., Wang, R.Z., Xu, Y.X., 2002. Study of solar powered solid adsorption desiccant cooling system used for grain storage. *Renewable Energy*, 25, pp. 417-430.
- [14] Pahlavanzadeh, H., Mozaffari, H., 2003. Performance optimization of rotary desiccant dehumidifiers. *Iranian Journal of science and Technology*, 27, pp.337-344.
- [15] Pahlavanzadeh, H., Zamzamian, A.H., 2006. A mathematical model for a fixed desiccant bed dehumidifier concerning Ackermann correction factor. *Iranian Journal of science and Technology*, 30, pp. 1-9.
- [16] Lee, Y., Park, S., Kang, S., 2021. Performance analysis of a solid desiccant cooling system for a residential air conditioning system. *Appl. Therm. Eng.*, 182, pp. 1-8.
- [17] Yeboah, S.K., Darkwa, J., 2021. Experimental investigation into the integration of solid desiccant packed beds with oscillating heat pipes for energy efficient isothermal adsorption processes. *Thermal Sci. Eng. Progress*, 21, pp. 100791.
- [18] Yu, L., Shamim, J.A., Hsu, W., Daiguji, H., 2021. Optimization of parameters for air dehumidification systems including multilayer fixed-bed binder-free desiccant dehumidifier. *Int. J. Heat Mass Transfer*, 172, pp. 121.
- [19] De Antonellis, S., Colombo, L., Freni, A., Joppolo, C., 2021. Feasibility study of a desiccant packed bed system for air humidification. *Energy*, 214, pp. 119002.
- [20] Bhabhor, K.K., Jani, D.B., 2021. Performance analysis of desiccant dehumidifier with different channel geometry using CFD. *J. Build. Eng.*, 44, pp. 103021.
- [21] Awad, M.M., Hamed, A.H., Bekheit, M.M., 2008. Theoretical and experimental investigation on the radial flow desiccant dehumidification bed. *Appl. Therm. Eng.* 28, pp. 75-85.
- [22] Kabeel, A.E., 2009. Adsorption-desorption operations of multilayer desiccant packed bed for dehumidification applications. *Renewable Energy*, 34, pp. 255-265.
- [23] Abd-Elrahman, W.R., Hamed, A.H., El-Emam, S.H., Awad, M.M., 2011. Experimental investigation on the performance of radial flow desiccant bed using activated alumina. *Appl. Therm. Eng.*, 31, pp.2709-2715.
- [24] Hamed, A.H., Abd-Elrahman, W.R., El-Emam, S.H., Awad, M.M., 2013. Theoretical and experimental investigation on the transient coupled heat and mass transfer in a radial flow desiccant packed bed. *Energy Convers. Manage.*, 65, pp. 262-271.
- [25] Ramzy, A.K., Kadoli, R., TP, A.B., 2013. Experimental and theoretical investigations on the cyclic operation of TSA cycle for air dehumidification using packed beds of silica gel particles. *Energy*, 56, pp. 8-24.
- [26] Ramzy, A.K., AbdelMeguid, H., Elawady, W.M., 2015. A novel approach for enhancing the utilization of solid desiccants in packed bed via intercooling. *Appl. Therm. Eng.*, 78, pp. 82-89.
- [27] Finocchiaro, P., Beccali, M., Gentile, V., 2016. Experimental results on adsorption beds for air dehumidification. *Int. J. Refrig.*, 63, pp. 100-112.
- [28] Pistocchini, L., Garone, S., Motta, M., 2016. Air dehumidification by cooled adsorption in silica gel grains. Part I: Experimental development of a prototype. *Appl. Therm. Eng.*, 107, pp. 888-897.
- [29] Pistocchini, L., Garone, S., Motta, M., 2017. Air dehumidification by cooled adsorption in silica gel grains. part ii: theoretical analysis of the

- prototype testing results. *Appl. Therm. Eng.*, 110, pp.1682–1689.
- [30] Shamim, J.A., Hsu, W.L., Kitaoka, K., Paul, S., Daiguji, H., 2018. Design and performance evaluation of a multilayer fixed-bed binder-free desiccant dehumidifier for hybrid air-conditioning systems: part i–experimental. *Int. J. Heat Mass Transfer*, 116, pp. 1361–1369.
- [31] Hsu, W.L., Paul, S., Shamim, J.A., Kitaoka, K., Daiguji, H., 2018. Design and performance evaluation of a multilayer fixed-bed binder-free desiccant dehumidifier for hybrid air-conditioning systems: part II–theoretical analysis. *Int. J. Heat Mass Transfer*, 116, pp. 1370–1378.
- [32] Yeboah, S.K., Darkwa, J., 2019. Experimental investigations into the adsorption enhancement in packed beds using Z-Annular flow configuration. *Int. J. Therm. Sci.*, 136, pp.121–134.
- [33] Abd-Elhady, M.M., Salem, M.S., Hamed, A.M., EL-Sharkawy, I.I., 2022. Solid desiccant-based dehumidification systems: A critical review on configurations, techniques, and current trends. *Int. J. of Refrigeration*, 133, pp.337–352.
- [34] Pahlavanzadeh, H., Zamzamian, S.A.H., Omidkhah Nasrin M.R., 2007. ANALYSIS OF EFFECTIVE PARAMETERS ON A ROTARY DESICCANT WHEEL PERFORMANCE. *MECHANICAL ENGINEERING SHARIF*, 23(40), pp. 155-162.
- [35] Zamzamian, S.A.H., Pahlavanzadeh, H., 2011. Theoretical and Experimental Investigation of the Key Components for a Rotary Desiccant Wheel. *Iranian Journal of Chemistry and Chemical Engineering (IJCCE)*, 30(3), pp. 25-30.
- [36] Ghaffarpasand O., 2018. Characterization of unsteady double-diffusive mixed convection flow with solet and dufour effects in a square enclosure with top moving lid. *Journal of Heat and Mass Transfer Research*, 5, pp. 51-68.
- [37] Winkelman JGM, Sijbring H, Beenackers AACM, De Vries E.T., 1992. Modeling and simulation of industrial formaldehyde absorbers. *Chemical Engineering Science*, 47, pp.3785-3792.